




Communication

Two New Fatty Acid Derivatives, Omphalotols A and B and Anti-*Helicobacter pylori* Fatty Acid Derivatives from Poisonous Mushroom *Omphalotus japonicus*

Seulah Lee ^{1,2,†}, Tae Wan Kim ^{1,†}, Yong Hoon Lee ¹, Dong-Min Kang ³ , Rhim Ryoo ⁴, Yoon-Joo Ko ⁵, Mi-Jeong Ahn ³  and Ki Hyun Kim ^{1,*} 

¹ School of Pharmacy, Sungkyunkwan University, Suwon 16419, Korea; seulah@kopri.re.kr (S.L.); asde8282@naver.com (T.W.K.); yhl2090@naver.com (Y.H.L.)

² Division of Life Sciences, Korea Polar Research Institute, KIOST, Incheon 21990, Korea

³ College of Pharmacy and Research Institute of Pharmaceutical Sciences, Gyeongsang National University, Jinju 52828, Korea; kdm7105@gnu.ac.kr (D.-M.K.); amj5812@gnu.ac.kr (M.-J.A.)

⁴ Special Forest Products Division, Forest Bioresources Department, National Institute of Forest Science, Suwon 16631, Korea; rryoo@korea.kr

⁵ Laboratory of Nuclear Magnetic Resonance, National Center for Inter-University Research Facilities (NCIRF), Seoul National University, Gwanak-gu, Seoul 08826, Korea; yjko@snu.ac.kr

* Correspondence: khkim83@skku.edu; Tel.: +82-31-290-7700

† These authors contributed equally to this study.



Citation: Lee, S.; Kim, T.W.; Lee, Y.H.; Kang, D.-M.; Ryoo, R.; Ko, Y.-J.; Ahn, M.-J.; Kim, K.H. Two New Fatty Acid Derivatives, Omphalotols A and B and Anti-*Helicobacter pylori* Fatty Acid Derivatives from Poisonous Mushroom *Omphalotus japonicus*. *Pharmaceuticals* **2022**, *15*, 139. <https://doi.org/10.3390/ph15020139>

Academic Editor: Grażyna Zgórk

Received: 13 December 2021

Accepted: 23 January 2022

Published: 25 January 2022

Publisher's Note: MDPI stays neutral with regard to jurisdictional claims in published maps and institutional affiliations.



Copyright: © 2022 by the authors. Licensee MDPI, Basel, Switzerland. This article is an open access article distributed under the terms and conditions of the Creative Commons Attribution (CC BY) license (<https://creativecommons.org/licenses/by/4.0/>).

Abstract: As part of ongoing systematic research into the discovery of bioactive secondary metabolites with novel structures from Korean wild mushrooms, we investigated secondary metabolites from a poisonous mushroom, *Omphalotus japonicus* (Kawam.) Kirchn. & O. K. Mill. belonging to the family Marasmiaceae, which causes nausea and vomiting after consumption. The methanolic extract of *O. japonicus* fruiting bodies was subjected to the fractionation by solvent partition, and the CH₂Cl₂ fraction was analyzed for the isolation of bioactive compounds, aided by an untargeted liquid chromatography mass spectrometry (LC–MS)-based analysis. Through chemical analysis, five fatty acid derivatives (1–5), including two new fatty acid derivatives, omphalotols A and B (1 and 2), were isolated from the CH₂Cl₂ fraction, and the chemical structures of the new compounds were determined using 1D and 2D nuclear magnetic resonance (NMR) spectroscopy and high resolution electrospray ionization mass spectrometry (HR-ESIMS), as well as fragmentation patterns in MS/MS data and chemical reactions followed by the application of Snatzke's method and competing enantioselective acylation (CEA). In the anti-*Helicobacter pylori* activity test, compound 1 showed moderate antibacterial activity against *H. pylori* strain 51 with 27.4% inhibition, comparable to that of quercetin as a positive control. Specifically, compound 3 exhibited the most significant antibacterial activity against *H. pylori* strain 51, with MIC₅₀ and MIC₉₀ values of 9 and 20 μM, respectively, which is stronger inhibitory activity than that of another positive control, metronidazole (MIC₅₀ = 17 μM and MIC₉₀ = 46 μM). These findings suggested the experimental evidence that the compound 3, an α,β-unsaturated ketone derivative, could be used as a moiety in the development of novel antibiotics against *H. pylori*.

Keywords: *Omphalotus japonicus*; Marasmiaceae; fatty acid derivatives; LC–MS/MS; anti-*H. pylori* activity

1. Introduction

Mushrooms have been used to treat various diseases in traditional medicine [1], and a number of pharmacological and phytochemical studies on mushrooms have demonstrated that they are rich sources of various bioactive compounds that exhibit beneficial immunomodulatory, antioxidant, and angiostatic activities, as well as cytotoxicity against cancers [1–5]. Based on this evidence, mushrooms have emerged as potential valuable sources of bioactive natural products; however, most studies have focused on medicinal

and edible mushrooms, and little is known regarding bioactive secondary metabolites produced from poisonous mushrooms.

As part of ongoing systematic research on Korean wild mushrooms for the discovery of bioactive secondary metabolites with novel structures [6], we investigated bioactive secondary metabolites from a poisonous mushroom; *Omphalotus japonicus* (Kawam.) Kirchn. & O. K. Mill. *O. japonicus* is an orange-to-brown-colored gilled mushroom belonging to the family Marasmiaceae, which is found in Japan and Eastern Asia. It is a member of the genus *Omphalotus*, the members of which have bioluminescent fruit bodies that glow in dark [7]. This poisonous mushroom causes nausea and vomiting after consumption. Sesquiterpenoids have been identified as the major secondary metabolites in *O. japonicus*, the most well-known of which is illudin S, a representative toxic metabolite that exhibits potent cytotoxic and antiviral activities [8]. It has also displayed strong in vitro and in vivo antitumor activity against multi-drug-resistant tumors, and a novel anticancer drug, irofulven, was developed based on the structure and anticancer activity of illudin S [9–13]. Additionally, the potent cytotoxicity of illudin S has extended its application to other pharmacological effects, where its antiviral activity in an HSV-I/CV-1 assay and glutathione reductase inhibition have been confirmed [8,13,14]. Toxic illudane-type sesquiterpenes from *O. japonicus*, including dihydroilludin S and neoilludins A and B, have also been reported [15,16]. As other secondary metabolites, the luminescent substances, lampteroflavin [17], lamptero [18] have been identified from this mushroom, and polysaccharides [19] from *O. japonicus* have been reported to show antitumor activities.

In the present study, we conducted the fractionation of the methanolic extract of *O. japonicus* fruiting bodies, and chemical analysis of CH₂Cl₂ fraction was carried out to isolate potential bioactive compounds aided by an untargeted liquid chromatography-tandem mass spectrometry (LC–MS/MS)-based analysis. Five fatty acid derivatives (1–5), including two new fatty acid derivatives, omphalotols A and B (1 and 2), were isolated from the CH₂Cl₂ fraction. Herein, we describe the isolation and structural determination of compounds 1–5, and evaluate their anti-*H. pylori* activity.

2. Results and Discussion

2.1. Extraction of *O. japonicus* and Isolation of Compounds

Dried *O. japonicus* fruiting bodies were extracted with 80% methanol, and the crude methanolic extract was extracted by rotary evaporation. The resultant MeOH extract was sequentially applied to solvent partitioning using *n*-hexane, dichloromethane (CH₂Cl₂), ethyl acetate (EtOAc), and *n*-butanol (BuOH) as four organic solvents with increasing polarity. As a result, four main solvent fractions were obtained: *n*-hexane, CH₂Cl₂, EtOAc, and BuOH-soluble fractions. Based on the data from LC/MS and thin-layer chromatography (TLC) analysis for the four solvent fractions where major peaks characteristic of fatty acid derivatives were observed in CH₂Cl₂-soluble fraction, the CH₂Cl₂ fraction was subjected to chemical analysis since the fatty acid derivatives from *O. japonicus* have rarely been investigated in terms of their chemical constituents. The chemical analysis using sequential column chromatography, as well as preparative and semi-preparative HPLC, resulted in the isolation of five fatty acid derivatives (1–5) (Figure 1).

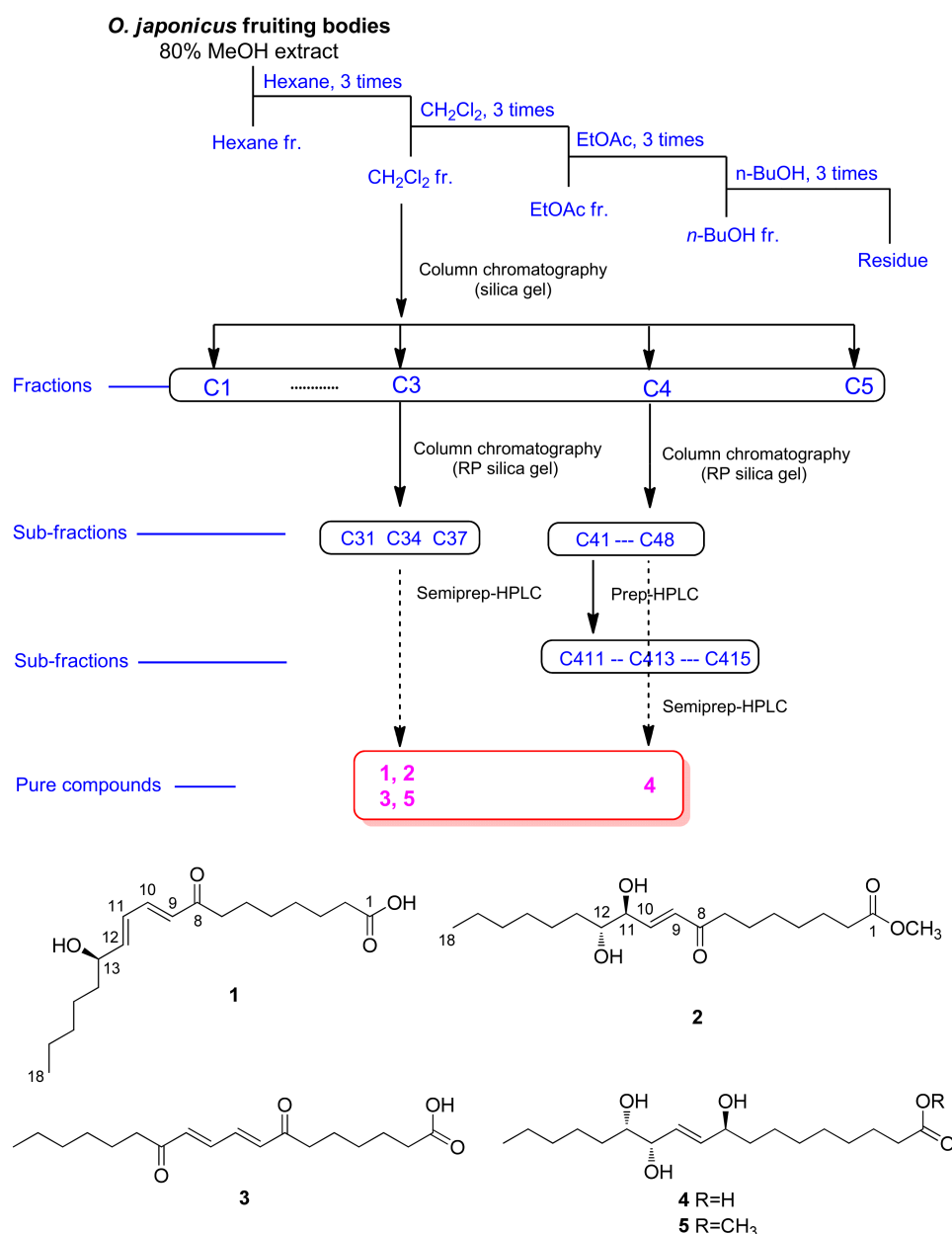


Figure 1. Separation scheme (top) and chemical structures (bottom) of compounds 1–5.

2.2. Structural Elucidation of the Isolated Compounds 1–5

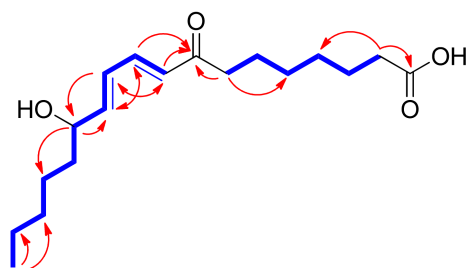
Compound 1 was isolated as a colorless oil. The molecular formula was established as $C_{18}H_{30}O_4$ from the molecular ion peak $[M + H]^+$ at m/z 311.2214 (calcd. for $C_{18}H_{31}O_4$, 311.2222) in the positive-ion mode of the HR-ESIMS. As shown in Table 1, the 1H NMR spectrum of 1 showed signals for olefinic protons at δ_H 7.27 (1H, dd, $J = 15.5, 11.0$ Hz), 6.41 (1H, dd, $J = 15.0, 11.0$ Hz), 6.25 (1H, dd, $J = 15.0, 6.0$ Hz), and 6.20 (1H, d, $J = 15.5$ Hz), an oxygenated methine at δ_H 4.17 (1H, q, $J = 6.0$ Hz), a terminal methyl group at δ_H 0.91 (3H, t, $J = 7.0$ Hz), deshielded methylenes at δ_H 2.62 (2H, t, $J = 7.5$ Hz) and 2.27 (2H, t, $J = 7.5$ Hz), and overlapping signals corresponding to the remaining methylenes from 1.33 to 1.60 ppm. The ^{13}C NMR data of 1 (Table 1) obtained by the aid of heteronuclear single quantum coherence (HSQC) spectrum showed four olefinic carbons (δ_C 147.0, 142.8, 128.9, and 127.3), an oxygenated carbon (δ_C 71.1), a terminal methyl carbon (δ_C 13.0), and the remaining carbons attributable to methylenes (δ_C 22.2 to 39.5). The above NMR data provided sufficient evidence to show that compound 1 is a fatty acid derivative [20].

Table 1. ^1H and ^{13}C NMR data for compounds **1** and **2** (δ ppm)^a.

Position	1		2	
	δ_{H} (J in Hz)	δ_{C}	δ_{H} (J in Hz)	δ_{C}
1		177.0		174.3
2	2.27 t (7.5)	33.9	2.30 t (7.5)	34.0
3	1.60 m ^b	24.3	1.62 m ^b	24.4
4	1.35 m ^b	28.5	1.31 m ^b	28.8
5	1.35 m ^b	28.5	1.31 m ^b	31.6
6	1.60 m ^b	24.3	1.62 m ^b	24.4
7	2.62 t (7.5)	39.5	2.57 t (7.5)	40.7
8		202.2		200.5
9	6.20 d (15.5)	128.9	6.38 dd (16.0, 1.5)	130.4
10	7.27 dd (15.5, 11.0)	142.8	6.81 dd (16.0, 5.0)	142.6
11	6.41 dd (15.0, 11.0)	127.3	4.32 ddd (5.0, 3.5, 1.5)	74.2
12	6.25 dd (15.0, 6.0)	147.0	3.79 m	74.0
13	4.17 q (6.0)	71.1	1.43 m	32.1
14	1.54 m	36.5	1.31 m ^b	28.8
15	1.35 m ^b	24.8	1.31 m ^b	25.2
16	1.33 m ^b	22.2	1.31 m ^b	22.5
17	1.33 m ^b	31.7	1.31 m ^b	31.6
18	0.91 t (7.0)	13.0	0.90 t (7.0)	13.9
1-OCH ₃			3.67 s	51.3

^a 700 MHz in CD₃OD for **1** and 850 MHz in CDCl₃ for **2**; coupling constants (in Hz) are in parentheses. Assignments were based on the HSQC, HMBC, and TOCSY/ ^1H - ^1H COSY spectra. ^b Overlapped.

With the splitting patterns of the olefinic protons, the location of the olefinic groups as well as the hydroxyl group could be estimated as shown in Figure 1, and they were determined to be *trans*-orientated based on the *J* values of 15.0 Hz and 15.5 Hz [20]. This was also confirmed by HMBC correlations of H-9/C-11 (δ_{C} 127.3), H-10/C-12 (δ_{C} 147.0), H-11/C-9 (δ_{C} 128.9) and C-13 (δ_{C} 71.1), and H-12/C-10 (δ_{C} 142.8), as well as the spin systems observed in the total correlation spectroscopy (TOCSY) spectrum for C-9-C-10-C-11-C-12-C-13 (Figure 2). The HMBC correlations of H-10/C-8 (δ_{C} 202.2), H-9/C-8, and C-7 (δ_{C} 39.5) determined a carbonyl group at C-8, and those of H₂-2/C-1 (δ_{C} 177.0) and C-4, H₂-7/C-5, H₃-18/C-17, and C-16, along with cross-peaks observed in the TOCSY spectrum for the spin systems of C-2-C-3-C-4-C-5-C-6-C-7 and C-13-C-14-C-15-C-16-C-17-C-18 determined the remaining gross structure of **1** (Figure 2). The characterized chemical structure of **1** was confirmed by MS/MS analysis, where the MS² of **1** yielded *m/z* 293.2, 157.0, and 101.0 (Figure S7).

**Figure 2.** TOCSY (bold lines) and key HMBC (arrows) correlations of **1**.

To assign the absolute configuration of the hydroxyl group at C-13, chemical-derivative method developed by our group, using competing enantioselective acylation (CEA) coupled with LC/MS analysis [21], was utilized. The rates of parallel reactions with the homobenzotetramisole (HBTM) catalysts were compared using LC/MS. Two sets of compound **1** (each 0.2 mg) and *S*- and *R*-HBTM catalysts (each 0.1 mg) were reacted for each parallel acylation reaction. Samples of each reaction were quantitatively analyzed using LC/MS to measure the reaction rate catalyzed by *S*- and *R*-HBTM. The acylated derivative

(1A, $[M + Na]^+$ peak at m/z 389), esterified by propionic anhydride in the hydroxyl group at C-13, was expected as a result of the CEA reaction (Figure 3). The anticipated derivatives were detected in samples of both parallel reactions, and the esterification reaction with *S*-HBTM was faster than that with *R*-HBTM (Figures 3 and S8), suggesting that compound 1 has a 13*R*-configuration according to the mnemonic to predict the configuration of secondary alcohols in the CEA reaction (Figure 3). Accordingly, the complete structure of compound 1 was determined to be (13*R*)-8-oxo-octadeca-(9*E*,11*E*) dienoic acid and named omphalotol A.

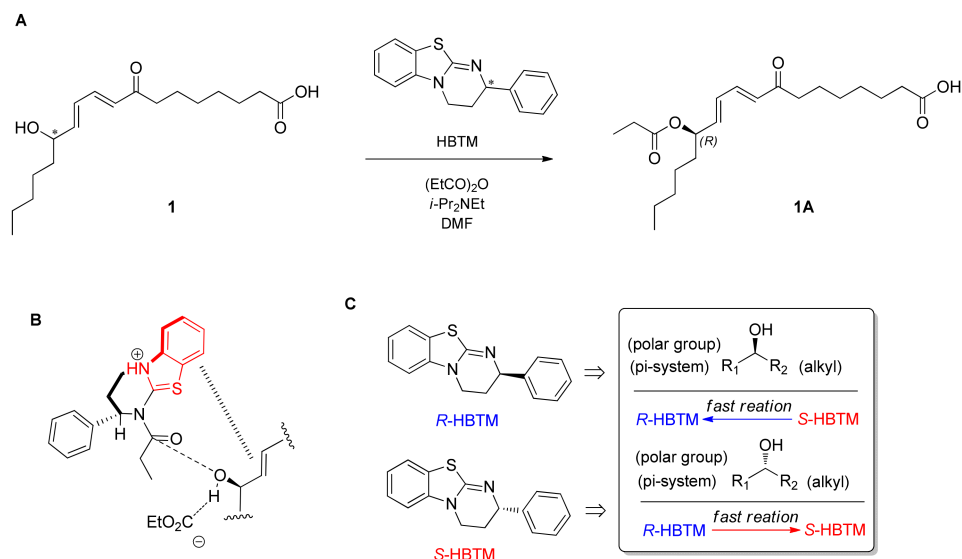


Figure 3. (A) CEA reaction for the determination of absolute configuration of compound 1. (B) Proposed favorable transition state of compound 1 in the reaction. (C) Mnemonic to predict the configuration of secondary alcohols in CEA reaction. * defines the chiral center.

Compound 2 was obtained as a colorless oil. The molecular formula was determined to be $C_{19}H_{34}O_5$ from the molecular ion peak $[M - H]^-$ at m/z 341.2294 (calcd. for $C_{19}H_{33}O_5$, 341.2328) in the negative-ion mode of HR-ESIMS. The 1H NMR spectrum of 2 (Table 1) showed signals of a pair of olefinic protons at δ_H 6.81 (1H, dd, $J = 16.0, 5.0$ Hz) and 6.38 (1H, dd, $J = 16.0, 1.5$ Hz), two oxygenated methines at δ_H 4.32 (1H, ddd, $J = 5.0, 3.5, 1.5$ Hz) and 3.79 (1H, m), a methoxyl group at δ_H 3.67 (3H, s), a terminal methyl group at δ_H 0.90 (3H, t, $J = 7.2$ Hz), deshielded methylenes at δ_H 2.57 (2H, t, $J = 7.4$ Hz) and 2.30 (2H, t, $J = 7.5$ Hz), and overlapping signals attributable to the remaining methylenes from 1.31 to 1.62 ppm. The ^{13}C NMR data of 2 (Table 1) obtained by the assistance of the HSQC spectrum exhibited two olefinic carbons (δ_C 142.6, 130.4), two oxygenated carbons (δ_C 74.2, 74.0), a methoxyl carbon (δ_C 51.3), a terminal methyl carbon (δ_C 13.9), and the rest of the carbon signals attributable to methylenes (δ_C 22.5 to 40.7).

The coupling constants of the olefinic protons of H-9 ($J = 16.0, 1.5$ Hz), H-10 ($J = 16.0, 5.0$ Hz), and the oxygenated methine of H-11 ($J = 5.0, 3.5, 1.5$ Hz) supported the *E* configuration of the double bond and the existence of one hydroxyl group next to the olefinic group (Figure 1). The HMBC correlations of H-9/C-11 (δ_C 74.2), H-9/C-8 (δ_C 200.5), H-10/C-8, H-10/C-11, H-10/C-12 (δ_C 74.0), and H-11/C-9 (δ_C 130.4), as well as spin systems of C-9-C-10-C-11-C-12-C-13 observed in the 1H - 1H COSY spectrum (Figure 4) further support the above prediction and complete the “A” partial structure of 2, as shown in Figure 4. The HMBC correlations of 1-OCH₃/C-1 (δ_C 174.3), H₂-2/C-1, and H₂-3/C-1 determined another “B” partial structure of 2 (Figure 4). The complete planar structure of 2, including the locations of the olefinic and hydroxyl groups, was determined by MS/MS analysis, where the MS² of 2 yielded m/z 241.1 and 171.1 (Figure S15).

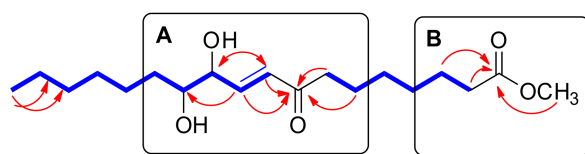


Figure 4. ^1H - ^1H COSY (bold lines) and key HMBC (arrows) correlations of **1**.

The absolute configurations of C-11 and C-12 were determined by employing Snatzke's method [22,23] and the observed J value. The small coupling constant ($J = 3.5$ Hz) between H-11 and H-12 indicated the *erythro* configuration of the vicinal diol in **2** [24]. To assign the absolute configuration, a ligand–metal complex was generated by mixing compound **2** and dimolybdenum tetraacetate $[\text{Mo}_2(\text{OAc})_4]$ as an auxiliary chromophore, for which the induced circular dichroism (ICD) spectrum was recorded [25]. Based on Snatzke's rule, the Cotton effect at approximately 310 nm reflects the torsional angle of the O-C-C-O moiety of a 1,2-diol derivative in the $[\text{Mo}_2(\text{OAc})_4]$ -ICD spectrum [22]. As shown in Figure 5, the negative ICD at 310 nm corresponds to a negative torsional angle of the O-C-C-O moiety in the favored conformation (**2A**), which allowed the assignment of the (11*S*,12*R*)-form among the possible *erythro* configurations, (11*S*,12*R*) or (11*R*,12*S*). Compound **2** was characterized as methyl (11*S*,12*R*)-8-oxo-(9*E*)-octadecenoate and named omphalotol B (Figure 1).

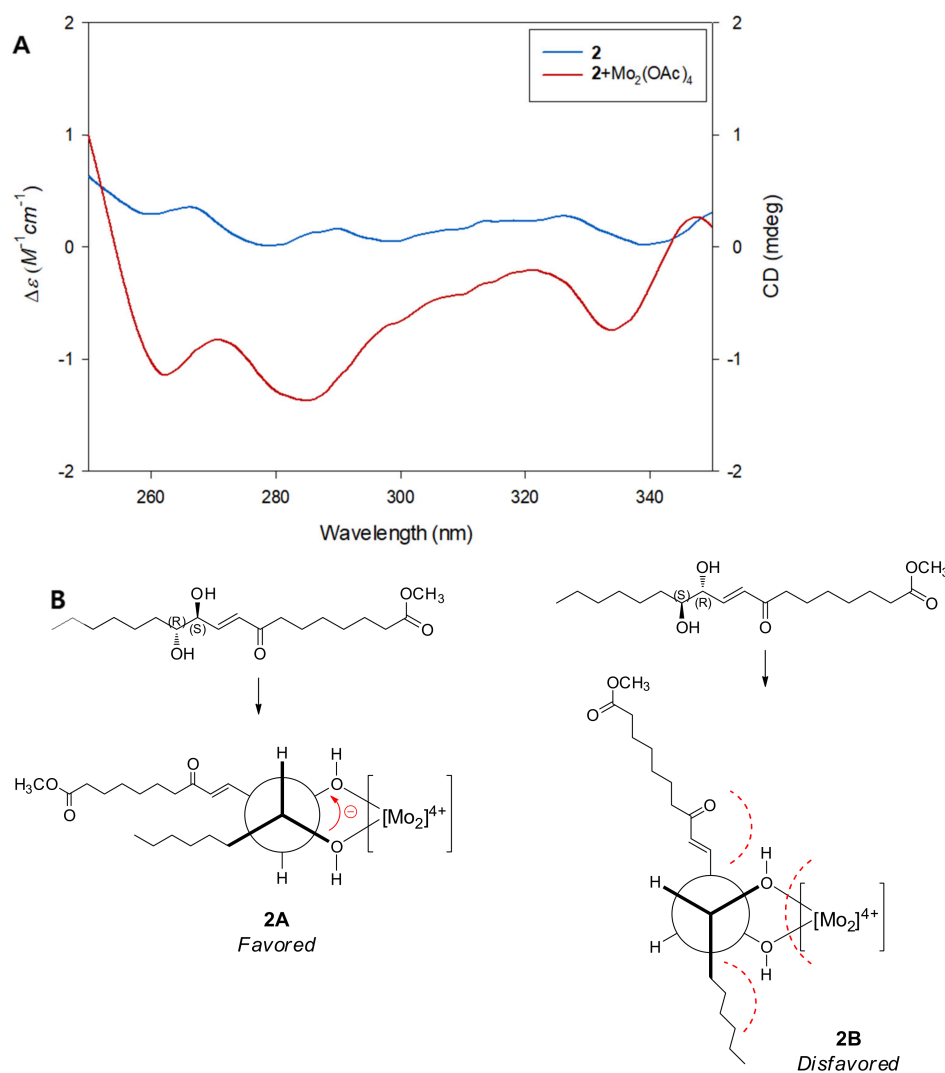


Figure 5. Determination of absolute configurations of C-11 and C-12 in compound **2** according to Snatzke's method. (A) ECD spectrum of **2** and induced ECD spectrum of in situ formed Mo-complex of **2** recorded in DMSO. (B) Favored conformations of Mo-complex of **2**.

The known compounds were identified as (8*E*,10*E*)-7,12-dioxo-8,10-octadecadienoic acid (3) [26], pinellic acid (4) [27] and methyl (9*S*,12*S*,13*S*)-trihydroxy-10*E*-octadecenoate (5) [28], by comparing their NMR spectroscopic and physical data with those previously reported, along with LC/MS analysis.

2.3. Antibacterial Activity Evaluation of Isolated Compounds against *H. pylori*

H. pylori is a Gram-negative and microaerophilic bacterium, which causes major public health problems worldwide, affecting approximately 50% of the global population [29]. Eradication of *H. pylori* leads to resolution of both gastritis and gastric ulcers, and even gastric cancer [30]. Although a combination prescription of antibiotics with a proton pump inhibitor is effective, the efficacy has decreased mainly due to the increasing resistance of *H. pylori* strains against antibiotics such as clarithromycin and metronidazole [31–34]. Therefore, there has been a pressing need to look for new compounds, which can overcome this resistance and provide an effective therapy against *H. pylori* infection. Natural products with less adverse effects can be alternative approaches for the intervention of gastric disorders caused by this bacterium. The isolated compounds 1–5 were tested for their antibacterial activity against *H. pylori* strain 51 at the final concentration of 100 μ M (Table 2). Among the isolates, compound 1 showed moderate antibacterial activity against *H. pylori* strain 51 with 27.4% inhibition, comparable to that of quercetin as a positive control. Specifically, compound 3 exhibited the most significant antibacterial activity against the strain with 97.5% inhibition (Table 2). Its inhibitory activity, with the minimal inhibitory concentrations (MIC)₅₀ and MIC₉₀ values of 9 and 20 μ M, respectively, was more potent than those of a positive control and metronidazole (MIC₅₀ = 17 μ M and MIC₉₀ = 46 μ M). In addition, the minimum bactericidal concentration (MBC) values of compound 3 and metronidazole were 12.5 and 12.5 μ M, respectively. The other compounds failed to show anti-*H. pylori* activity. Based on these findings, it is suggested that the α,β -unsaturated carbonyl moiety of compound 3 can play a role in the inhibition of *H. pylori* growth, and the hydroxyl group of compound 2 may decrease the activity. *H. pylori* produces a urease which catalyzes the hydrolysis of urea to produce ammonia for neutralizing the acidic condition of the stomach. It has been known that simple α,β -unsaturated ketones inhibited urease activity by binding to the cysteinyl residue in the active sites of the enzyme [35]. Further study is required to elucidate the exact mechanism of compound 3 to inhibit the growth of *H. pylori*. Specificity to *H. pylori* and toxicity to other cells of this compound are also required in the following study.

Table 2. Anti-*H. pylori* activity of compounds 1–5.

Compound	Concentration (μ M)	Inhibition (%)	MIC (μ M)	MIC ₅₀ (μ M)	MIC ₉₀ (μ M)
1		27.4 \pm 4.5 ^b			
2		11.1 \pm 0.3 ^c			
3	100	97.5 \pm 0.8 ^a	3.1	9	20
4		2.5 \pm 0.8 ^d			
5		0.2 \pm 0.1 ^d			
Quercetin *	100	34.4 \pm 0.6 ^b	50		
Metronidazole *		97.0 \pm 0.1 ^a	6.3	17	46

* Positive controls. Data are presented as mean \pm SD of experiments in duplicates. Different upper letters in the same column indicate a significant difference ($p < 0.05$) among the samples.

3. Materials and Methods

3.1. General Experimental Procedure

The information on general experimental procedure is provided in Supplementary Materials.

3.2. Mushroom Material

Fresh fruiting bodies of *O. japonicus* were collected from Pocheon, Gyeonggi-do, Korea in September 2019. This material was identified by DNA analysis, depending on the modified method [36]. The fungal-specific PCR primers ITS1 and ITS4 were used to amplify the internal transcribed spacer (ITS) region according to a modified method [37]. This sequence homology corresponded to that of *O. japonicus* (syn. *Omphalotus guepiniiformis*), with the highest matching score in the NCBI BLAST network server. A voucher specimen (SKKU-HK-2019-09) of the mushroom was deposited at the herbarium of the School of Pharmacy, Sungkyunkwan University, Korea.

3.3. Extraction of *O. japonicus* and Isolation of Compounds

The dried fruiting bodies of *O. japonicus* (0.6 kg) were extracted with 80% aqueous MeOH three times (each 3 L × 24 h) at room temperature. The resultant extracts were filtered, and the filtrate was evaporated under reduced pressure using a rotary evaporator to obtain a crude MeOH extract (43.6 g). The extract was suspended in distilled water (700 mL) and MeOH (30 mL) and successively solvent-partitioned three times with *n*-hexane, dichloromethane, ethyl acetate, and *n*-butanol, yielding soluble layers of *n*-hexane (6.3 g), CH₂Cl₂ (6.7 g), EtOAc (2.4 g), and *n*-butanol (15.6 g). The CH₂Cl₂ fraction (6.7 g) was subjected to silica gel column chromatography (CC) (a gradient solvent system; CH₂Cl₂/MeOH, from 70:1 to 1:1) to yield five fractions (Fr. C1–C5). Fr. C3 (1.2 g) was subjected to reverse phase (RP) C₁₈ CC to yield seven subfractions (Fr. C31–C37). Fr. C34 (91.2 mg) was purified by semi-preparative HPLC (MeOH/H₂O, 67:33) to give compounds **5** (*t*_R 19.0 min, 2.2 mg), **1** (*t*_R 23.5 min, 3.6 mg), **2** (*t*_R 37.0 min, 1.3 mg), and **3** (*t*_R = 39.5 min, 0.3 mg). Fr. C4 (1.7 g) was subjected to RP-C₁₈ CC, yielding eight subfractions (Fr. C41–C48). Fr. C41 (203.4 mg) was fractionated using preparative HPLC (a gradient solvent system; MeOH/H₂O, from 50:50 to 100:0), which yielded five subfractions (Fr. C411–C415). Fr. C413 (61.5 mg) was purified using semi-preparative HPLC (MeOH/H₂O, 54:46) to yield compound **4** (*t*_R 35.0 min, 1.8 mg).

3.3.1. Omphalotol A (**1**)

Colorless oil; $[\alpha]_D^{25} -2.7$ (*c* 0.07, MeOH); UV (MeOH) λ_{\max} (log ϵ) 270 (3.4) nm; IR (KBr) ν_{\max} : 3385, 2950, 2831, 1722, 1030 cm⁻¹; ¹H and ¹³C NMR spectroscopic data, see Table 1; (+)-HR-ESIMS *m/z* 311.2214 [M + H]⁺ (calcd. for C₁₈H₃₁O₄, 311.2222).

3.3.2. Omphalotol B (**2**)

Colorless oil; $[\alpha]_D^{25} +30.5$ (*c* 0.07, MeOH); UV (MeOH) λ_{\max} (log ϵ) 215 (2.6) nm; IR (KBr) ν_{\max} : 3371, 2864, 1710, 1018 cm⁻¹; ECD (MeOH) λ_{\max} ($\Delta\epsilon$) 245 (+0.3), 268 (+0.3), 292 (+0.1), 328 (+0.3) nm; ¹H and ¹³C NMR spectroscopic data, see Table 1; (–)-HR-ESIMS *m/z* 341.2294 [M – H][–] (calcd. for C₁₉H₃₃O₅, 341.2328).

3.4. MS/MS Analysis of Compounds **1** and **2**

Stock solutions of compounds **1** and **2** were prepared by dissolving 0.1 mg of sample in 200 μ L MeOH. The solution was further diluted with MeOH, filtered through a 0.45- μ m hydrophobic PTFE filter, and finally analyzed by LC/MS/MS, Agilent 1290 Infinity II series with 6545 LC/quadrupole time of flight (Q-TOF) mass spectrometer (Agilent Technologies). Analysis was performed by injecting 1 μ L of the sample using an Agilent Eclipse Plus C₁₈ RRHD (1.8 μ m, 2.1 × 50 mm) set at 30 °C. The mobile phase consisting of formic acid in H₂O (0.1% (*v/v*)) (A) and formic acid in acetonitrile (0.1% (*v/v*)) (B) was delivered at a flow rate of 0.3 mL/min by applying the following programmed gradient elution: 0–3.0 min, 10% (B); 3.0–10.0 min, 10–100% (B); 10.0–12.0 min, 100% (B); 12.0–15.0 min, 10% (B). The

MS system was equipped with an ESI source and operated in both negative and positive ionization modes with a data acquisition range from 100 to 600 m/z .

3.5. Experimental Procedures to Determine the Absolute Configuration of Compound 1

3.5.1. CEA Reaction

Parallel reactions for the CEA reaction were performed as reported by Lee et al. [21], using *S*- and *R*-HBTM. Compound 1 (0.5 mg, 1.61 μmol) was transferred to two transparent, capped 5 mL vials at room temperature, and dimethylformamide (DMF) (90 μL) was added as the organic solvent for the CEA reaction. Both *S*- and *R*-HBTM (10 μL , 0.38 μmol) were added, and *N,N*-diisopropylethylamine (1.0 μL , 5.3 μmol) was successively transferred. Propionic anhydride (0.6 μL , 5.3 μmol) was added to start the CEA reaction. After 10 min, 2 μL aliquots from each reaction were acquired for LC/MS analysis and quenched with 98 μL of MeOH to make a total volume of 100 μL .

3.5.2. LC/MS Analysis

An aliquot (5 μL) of the sample (100 μL) acquired from each parallel reaction was directly injected into the LC/MS (Phenomenex Luna C₁₈, 4.6 \times 100 mm, 3.5 μm , flow rate: 0.3 mL/min; Torrance, CA, USA), and full scans in positive- and negative-ion modes (scan range m/z 100–1000) were applied to identify the desired acylated derivative. The mobile phase consisted of 0.1% (*v/v*) formic acid in distilled water (A) or acetonitrile (B) with a gradient solvent system as follows: 10–100% B for 10 min, 100% B (isocratic) for 5 min, and then 10% B (isocratic) for 5 min for the post-run washing procedure of the column. The reaction rate catalyzed by both *S*- and *R*-HBTM was determined by measuring the peak areas of the acylated derivatives.

3.6. Absolute Configuration of the 1,2-diol Functionalities in Compound 2

According to a published procedure [22,23], 2 (0.5 mg) and Mo₂(OAc)₄ (0.75 mg) were mixed in 1.0 mL of dry DMSO with a ligand-to-metal molar ratio of approximately 1.0:1.2, and the solution was directly subjected to ECD measurements. The first circular dichroism (CD) spectrum was recorded immediately after mixing, and its time evolution was monitored until it was stationary (approximately 30 min after mixing). The inherent CD was subtracted. The observed signs of the diagnostic band at approximately 310 nm in the induced CD spectra were correlated with the absolute configuration of the 1,2-diol moiety.

3.7. Anti-*Helicobacter pylori* Activity

A clinical strain of *H. pylori* 51 isolated from a Korean patient with a duodenal ulcer (HPKTCC B0006) was provided by the *H. pylori* Korean Type Culture Collection, School of Medicine, Gyeongsang National University, Korea. The strain was grown and maintained on Brucella agar medium (BD Co., Sparks, MD, USA) supplemented with 10% horse serum (Gibco, New York, NY, USA). The culture conditions were 37 °C, 100% humidity, and 10% CO₂ for 2–3 days.

MICs were determined by the broth dilution method previously reported [38,39]. Twenty microliters of bacterial colony suspension equivalent to 2–3 \times 10⁸ cfu/mL and twenty microliters of two-fold diluted samples and controls were added to each well of a 6-well plate containing Brucella broth medium supplemented with 10% horse serum. The final volume was brought to 2 mL. After 24 h of incubation, bacterial growth was evaluated by measuring the optical density at 600 nm on a spectrophotometer (Optizen POP, Mecasys, Daejeon, Korea). MIC₅₀ and MIC₉₀ values were defined as the lowest concentrations of samples at which bacterial growth was inhibited by 50% and 90%, respectively, and were calculated using GraphPad Version 5.01 (GraphPad Software, Inc., San Diego, CA, USA).

MBC was determined by re-culturing broth dilution that inhibits the growth of *H. pylori* on the agar plate. Twenty microliter of broth dilution was streaked onto Brucella agar plate and incubated for 48 h. The MBC value was defined as the lowest concentration that showed no colonies of bacteria on agar plates.

3.8. Statistical Analysis

One-way analysis of variance was performed using Excel 2019 (Microsoft, Redmond, WA, USA). Values with $p < 0.05$ were considered statistically significant.

4. Conclusions

In this study, we isolated and identified five fatty acid derivatives (1–5), including two new fatty acid derivatives, omphalotols A and B (1 and 2), from the methanolic extracts of *O. japonicus* fruiting bodies. The structures of the new compounds were established using NMR spectroscopy and LC–MS analysis, as well as fragmentation patterns in MS/MS data and chemical reactions followed by the application of Snatzke's method and competing enantioselective acylation (CEA). In the anti-*H. pylori* activity test, we demonstrated that compound 1 showed moderate antibacterial activity against *H. pylori* strain 51 comparable to that of quercetin, a positive control. Specifically, compound 3 displayed the most significant anti-*H. pylori* activity with 97.5% inhibition, and its inhibitory activity with MIC₅₀ and MIC₉₀ values of 9 and 20 μ M, respectively, was more potent than those of metronidazole (MIC₅₀ = 17 μ M and MIC₉₀ = 46 μ M). Based on these findings, we conclude that compound 3, an α,β -unsaturated ketone derivative, could be used as a moiety in the development of novel antibiotics against *H. pylori*; however, further studies on its mechanism, antibacterial activity against another species, and toxicity to normal and cancerous cell lines are needed.

Supplementary Materials: The following are available online at <https://www.mdpi.com/article/10.3390/ph15020139/s1>; Figure S1: HR-ESIMS data of 1; Figure S2: UV spectrum of 1; Figure S3: ¹H NMR spectrum of 1 (CD₃OD, 700 MHz); Figure S4: HSQC spectrum of 1; Figure S5: HMBC spectrum of 1; Figure S6: TOCSY spectrum of 1; Figure S7: MS/MS analysis of 1 (MS² 333 [M + Na]⁺ → full-scan); Figure S8: LC/MS data of acylated derivative from CEA reaction of 1: (A) An acylated derivative of compound 1 in R-HBTM catalyzed acylation reaction; (B) An acylated derivative of compound 1 in S-HBTM catalyzed acylation reaction; Figure S9: HR-ESIMS data of 2; Figure S10: UV spectrum of 2; Figure S11: ¹H NMR spectrum of 2 (CDCl₃, 850 MHz); Figure S12: HSQC spectrum of 2; Figure S13: HMBC spectrum of 2; Figure S14: ¹H-¹H COSY spectrum of 2; Figure S15: MS/MS analysis of 2 (MS² 341 [M – H][−] → full-scan). General experimental procedure.

Author Contributions: Conceptualization, M.-J.A. and K.H.K.; formal analysis, S.L., T.W.K., Y.H.L., D.-M.K., R.R., Y.-J.K. and M.-J.A.; investigation, S.L., T.W.K., Y.H.L. and D.-M.K.; writing—original draft preparation, S.L. and K.H.K.; writing—review and editing, K.H.K.; visualization, S.L. and T.W.K.; supervision, M.-J.A. and K.H.K.; project administration, K.H.K.; funding acquisition, K.H.K. All authors have read and agreed to the published version of the manuscript.

Funding: This work was supported by a National Research Foundation of Korea (NRF) grant funded by the Korean government (MSIT; grant numbers 2019R1A5A2027340 and 2021R1A2C2007937).

Institutional Review Board Statement: Not applicable.

Informed Consent Statement: Not applicable.

Data Availability Statement: Not applicable.

Conflicts of Interest: The authors declare that they have no conflict of interest.

References

1. Patel, S.; Goyal, A. Recent Developments in Mushrooms as Anti-Cancer Therapeutics: A Review. *3 Biotech* **2012**, *2*, 1–15. [[CrossRef](#)] [[PubMed](#)]
2. Wasser, S.P. Current Findings, Future Trends, and Unsolved Problems in Studies of Medicinal Mushrooms. *Appl. Microbiol. Biotech.* **2011**, *89*, 1323–1332. [[CrossRef](#)] [[PubMed](#)]
3. Paterson, R.R.M.; Lima, N. Biomedical Effects of Mushrooms with Emphasis on Pure Compounds. *Biomed. J.* **2014**, *37*, 357–368. [[CrossRef](#)] [[PubMed](#)]
4. Lee, S.; Ryoo, R.; Choi, J.H.; Kim, J.-H.; Kim, S.-H.; Kim, K.H. Trichothecene and Tremulane Sesquiterpenes from a Hallucinogenic Mushroom *Gymnopilus junonius* and Their Cytotoxicity. *Arch. Pharm. Res.* **2020**, *43*, 214–223. [[CrossRef](#)] [[PubMed](#)]

5. Lee, S.R.; Yi, S.A.; Nam, K.H.; Ryoo, R.; Lee, J.; Kim, K.H. Pantheric Acids a–C from a Poisonous Mushroom, *Amanita pantherina*, Promote Lipid Accumulation in Adipocytes. *J. Nat. Prod.* **2019**, *82*, 3489–3493. [[CrossRef](#)]
6. Lee, S.; Lee, D.; Ryoo, R.; Kim, J.-C.; Park, H.B.; Kang, K.S.; Kim, K.H. Calvatianone, a Sterol Possessing a 6/5/6/5-Fused Ring System with a Contracted Tetrahydrofuran B-Ring, from the Fruiting Bodies of *Calvatia nipponica*. *J. Nat. Prod.* **2020**, *83*, 2737–2742. [[CrossRef](#)]
7. Aoki, S.; Aboshi, T.; Onodera, T.; Kimura, K.-i.; Arai, D.; Iizuka, Y.; Murayama, T. Omphaloprenol A: A New Bioactive Polyisoprenepolyol Isolated from the Mycelium of Poisonous Mushroom *Omphalotus japonicus*. *Biosci. Biotechnol. Biochem.* **2021**, *85*, 1364–1370. [[CrossRef](#)]
8. Uto, Y.; Sasaki, K.; Takahashi, M.; Morimoto, K.; Inoue, K. Application of High-Speed Countercurrent Chromatography for the Purification of High-Purity Illudin S from *Omphalotus japonicus*. *Anal. Sci.* **2019**, *35*, 789–792. [[CrossRef](#)]
9. Kelner, M.J.; McMorris, T.C.; Estes, L.; Rutherford, M.; Montoya, M.; Goldstein, J.; Samson, K.; Starr, R.; Taetle, R. Characterization of Illudin S Sensitivity in DNA Repair-Deficient Chinese Hamster Cells: Unusually High Sensitivity of Ercc2 and Ercc3 DNA Helicase-Deficient Mutants in Comparison to Other Chemotherapeutic Agents. *Biochem. Pharmacol.* **1994**, *48*, 403–409. [[CrossRef](#)]
10. Kelner, M.J.; McMorris, T.C.; Montoya, M.A.; Estes, L.; Rutherford, M.; Samson, K.M.; Taetle, R. Characterization of Cellular Accumulation and Toxicity of Illudin S in Sensitive and Nonsensitive Tumor Cells. *Cancer Chemother. Pharmacol.* **1997**, *40*, 65–71. [[CrossRef](#)]
11. Baekelandt, M. Irofulven (Mgi Pharma). *Curr. Opin. Investig. Drugs* **2002**, *3*, 1517–1526. [[PubMed](#)]
12. Amato, R.J.; Perez, C.; Pagliaro, L. Irofulven, a Novel Inhibitor of DNA Synthesis, in Metastatic Renal Cell Cancer. *Investig. New Drugs* **2002**, *20*, 413–417. [[CrossRef](#)] [[PubMed](#)]
13. Liu, X.; Sturla, S.J. Profiling Patterns of Glutathione Reductase Inhibition by the Natural Product Illudin S and Its Acylfulvene Analogues. *Mol. Biosyst.* **2009**, *5*, 1013–1024. [[CrossRef](#)] [[PubMed](#)]
14. Pietsch, K.E.; Van Midwoud, P.M.; Villalta, P.W.; Sturla, S.J. Quantification of Acylfulvene–and Illudin S–DNA Adducts in Cells with Variable Bioactivation Capacities. *Chem. Res. Toxicol.* **2013**, *26*, 146–155. [[CrossRef](#)] [[PubMed](#)]
15. Ichihara, A.; Shirahama, H.; Matsumoto, T. Dihydroilludin S, a New Constituent from *Lampteromyces japonicus*. *Tetrahedron Lett.* **1969**, *10*, 3965–3968. [[CrossRef](#)]
16. Kuramoto, M.; Tsukihara, T.; Ono, N. Neoilludins a and B, New Bioactive Components from *Lampteromyces japonicus*. *Chem. Lett.* **1999**, *28*, 1113–1114. [[CrossRef](#)]
17. Uyakul, D.; Isobe, M.; Goto, T. *Lampteromyces* Bioluminescence: 3. Structure of Lampteroflavin, the Light Emitter in the Luminous Mushroom, *L. japonicus*. *Bioorg. Chem.* **1989**, *17*, 454–460. [[CrossRef](#)]
18. Nakanishi, K.; Tada, M.; Yamada, Y.; Ohashi, M.; Komatsu, N.; Terakawa, H. Isolation of Lampterol, an Antitumour Substance from *Lampteromyces japonicus*. *Nature* **1963**, *197*, 292. [[CrossRef](#)]
19. Fukuda, K.; Uematsu, T.; Hamada, A.; Akiya, S.; Komatsu, N.; Okubo, S. The Polysaccharide from *Lampteromyces japonicus*. *Chem. Pharm. Bull.* **1975**, *23*, 1955–1959. [[CrossRef](#)]
20. Kim, K.-H.; Moon, E.-J.; Kim, S.-Y.; Lee, K.-R. Anti-Melanogenic Fatty Acid Derivatives from the Tuber-Barks of *Colocasia antiquorum* var. *esculenta*. *Bull. Korean Chem. Soc.* **2010**, *31*, 2051–2053. [[CrossRef](#)]
21. Lee, S.R.; Park, H.B.; Kim, K.H. Highly Sensitive, Simple, and Cost- and Time-Effective Method to Determine the Absolute Configuration of a Secondary Alcohol Using Competing Enantioselective Acylation Coupled with LC/MS. *Anal. Chem.* **2018**, *90*, 13212–13216. [[CrossRef](#)] [[PubMed](#)]
22. Di Bari, L.; Pescitelli, G.; Pratelli, C.; Pini, D.; Salvadori, P. Determination of Absolute Configuration of Acyclic 1, 2-Diols with Mo₂(Oac)₄.1. Snatzke's Method Revisited. *J. Org. Chem.* **2001**, *66*, 4819–4825. [[PubMed](#)]
23. Pan, L.; Acuña, U.; Li, J.; Jena, N.; Ninh, T.; Pannell, C.; Chai, H.; Fuchs, J.; Carcache De Blanco, E.J.; Soejarto, D.D.; et al. Bioactive Flavaglines and Other Constituents Isolated from *Aglaia perviridis*. *J. Nat. Prod.* **2013**, *76*, 394–404. [[CrossRef](#)] [[PubMed](#)]
24. Nagle, D.G.; Gerwick, W.H. Structure and Stereochemistry of Constanolactones Ag, Lactonized Cyclopropyl Oxylipins from the Red Marine Alga *Constantinea simplex*. *J. Org. Chem.* **1994**, *59*, 7227–7237. [[CrossRef](#)]
25. Liangyan, L.; Tao, F.; Zhenghui, L.; Jikai, L. Four New 2, 5-Disubstituted Furan Vicinal Diols from the Fungus *Ceriporia alachuana*. *Chin. J. Org. Chem.* **2017**, *37*, 1577–1581.
26. Hamburger, M.; Handa, S.S.; Cordell, G.A.; Kinghorn, A.D.; Farnsworth, N.R. Plant Anticancer Agents, Xliii.(E, E)-7, 12-Dioxo-Octadeca-8, 10-Dien-1-Oic Acid (Ostopanic Acid), a Cytotoxic Fatty Acid from *Ostodes paniculata*. *J. Nat. Prod.* **1987**, *50*, 281–283. [[CrossRef](#)]
27. Naidu, S.V.; Gupta, P.; Kumar, P. Enantioselective Syntheses of (–)-Pinellic Acid, A- and B-Dimorphecolic Acid. *Tetrahedron* **2007**, *63*, 7624–7633. [[CrossRef](#)]
28. Miura, A.; Kuwahara, S. A Concise Synthesis of Pinellic Acid Using a Cross-Metathesis Approach. *Tetrahedron* **2009**, *65*, 3364–3368. [[CrossRef](#)]
29. McGee, D.J.; George, A.E.; Trainor, E.A.; Horton, K.E.; Hildebrandt, E.; Testerman, T.L. Cholesterol Enhances *Helicobacter Pylori* Resistance to Antibiotics and LI-37. *Antimicrob. Agents Chemother.* **2011**, *55*, 2897–2904. [[CrossRef](#)]
30. Chey, W.D.; Wong, B.C. Practice Parameters Committee of the American College of Gastroenterology. American College of Gastroenterology Guideline on the Management of *Helicobacter Pylori* Infection. *Off. J. Am. Coll. Gastroenterol.* | ACG **2007**, *102*, 1808–1825. [[CrossRef](#)]

31. Tankovic, J.; Lamarque, D.; Lascols, C.; Soussy, C.J.; Delchier, J.C. Clarithromycin resistance of *Helicobacter pylori* has a major impact on the efficacy of the omeprazole-amoxicillin-clarithromycin therapy. *Pathol. Biol.* **2001**, *49*, 528–533. [[CrossRef](#)]
32. Wang, Y.-C.; Li, W.-Y.; Wu, D.-C.; Wang, J.-J.; Wu, C.-H.; Liao, J.-J.; Lin, C.-K. In vitro activity of 2-methoxy-1,4-naphthoquinone and stigmasta-7,22-diene-3b-ol from *Impatiens balsamina* L. against multiple antibiotic-resistant *Helicobacter pylori*. *Evid. Based. Complement. Altern. Med.* **2011**, *2011*, 704721.
33. An, B.G.; Moon, B.S.; Kim, H.J.; Lim, H.C.; Lee, Y.C.; Lee, G.; Kim, S.H.; Park, M.; Kim, J.B. Antibiotic resistance in *Helicobacter pylori* strains and its effect on *H. pylori* eradication rates in a single center in Korea. *Ann. Lab. Med.* **2013**, *33*, 415–419. [[CrossRef](#)] [[PubMed](#)]
34. Park, J.Y.; Dunbar, K.B.; Mitui, M.; Arnold, C.A.; Lam-Himlin, D.M.; Valasek, M.A.; Thung, I.; Okwara, C.; Coss, E.; Cryer, B.; et al. *Helicobacter pylori* clarithromycin resistance and treatment failure are common in the USA. *Dig. Dis. Sci.* **2016**, *61*, 2373–2380. [[CrossRef](#)]
35. Tanaka, T.; Kawase, M.; Tani, S. Urease inhibitory activity of simple α,β -unsaturated ketones. *Life Sci.* **2003**, *73*, 2985–2990. [[CrossRef](#)]
36. Lee, S.B.; Taylor, J.W. Isolation of DNA from fungal mycelia and single spores. In *PCR Protocols: A Guide to Methods and Applications*; Gelfand, D.H., Sninsky, J.J., White, T.J., Eds.; Academic Press: San Diego, CA, USA, 1990; pp. 282–287.
37. Gardes, M.; Bruns, T.D. ITS Primers with Enhanced Specificity for Basidiomycetes—Application to the Identification of Mycorrhizae and Rusts. *Molec. Ecol.* **1993**, *2*, 113–118. [[CrossRef](#)]
38. Khalil, A.A.K.; Park, W.S.; Lee, J.; Kim, H.J.; Akter, K.M.; Goo, Y.M.; Bae, J.Y.; Chun, M.S.; Kim, J.H.; Ahn, M.J. A new anti-*Helicobacter pylori* juglone from *Reynoutria japonica*. *Arch. Pharmacol. Res.* **2019**, *42*, 505–511. [[CrossRef](#)]
39. Wayne, P. *Reference Method for Broth Dilution Antifungal Susceptibility Testing of Yeasts*; approved standard; CLSI document M27-A3; Clinical and Laboratory Standards Institute: Wayne, PA, USA, 2008; Volume 28, pp. 6–12.